

## CHARACTERIZATION AND MEASUREMENT OF SILVER NANOPARTICLES FROM SALINE-TOLERANT MICROALGAE BY SCANNING ELECTRON MICROSCOPY

Yuvaraj Sampathkumar<sup>1\*</sup>, Elumalai Sanniyasi<sup>1</sup>, Mohana Priya Arumugam<sup>2</sup>, Pavithra Dhamodharan<sup>2</sup>, Selvaraj Palanisamy<sup>3</sup>, Vikram Godishala<sup>4</sup>, Madhusudhanan Jeyaraman<sup>5</sup>, Vijayabaskar Pandian<sup>6</sup> and Kaushik Thamichelvam<sup>7</sup>

<sup>1</sup>Department of Biotechnology, University of Madras, Guindy Campus, Chennai - 600 025, Tamilnadu, India.

<sup>2</sup>Department of School of Bio Sciences and Technology, VIT, Vellore – 632014, Tamilnadu, India

<sup>3</sup>Department of Biochemistry & Biotechnology, Annamalai University, Annamalai Nagar -608002, Tamilnadu, India.

<sup>4</sup>Department of Biotechnology, Ganapathi Degree College, Parakal-506164, Telangana, India

<sup>5</sup>Department of Biotechnology, Anand Institute of Higher Technology, Kazhipattur, Chennai-603003, Tamilnadu, India.

<sup>6</sup>Multi-Disciplinary Research Unit (MDRU), Government Theni Medical College & Hospital, Theni – 625 512, Tamilnadu, India.

<sup>7</sup>Department of Research and Development, Quantee Data Tech Pvt Ltd, Chennai - 600 086, Tamilnadu, India.

**Corresponding Author: Yuvaraj Sampathkumar**

Department of Biotechnology, University of Madras, Guindy Campus, Chennai - 600 025, Tamilnadu, India.

Article Received on 24/07/2022

Article Revised on 14/08/2022

Article Accepted on 04/09/2022

### ABSTRACT

Currently, researchers look to natural biological processes such using marine algae, to create dependable and ecofriendly methods for the synthesis of metallic nanoparticles (AgNPs), Using microalgae like *Nostoc* sp., *Lyngbya* sp., and *Phormidium* sp. we have examined the intracellular and extracellular biosynthesis of silver nanoparticles in this study. The microalgae extract contains a variety of active biomolecules, including superoxide dismutase (SOD), oxidase, reductase, NAD-dependent enzymes, lipid, carbohydrates, peptides, protein and pigment. These molecules play a significant role in the formation of nanoparticles and structures in the nanometer range, which is demonstrated by a change in the brown colour that denotes the synthesis of silver nanoparticles. Extracted biogenic silver nanoparticles and studies on their characterization are used in a scanning electron microscopy field to analyze a 2D and 3D topographical blueprint. There was a logical relationship between the efficiencies of micro algae in the production of silver nanoparticles and their graphical studies provide a support in the 3 D Luminance imaging technology, Contour map analysis, and micro valley network. The silver nanoparticles pattern was deposited on micro glass slide and imaged by SEM and EDS (FEI Quanta) with Digital Surf Mountain @ surface analysis technology to characterize the silver nanoparticles using electron beam lithography. According to the size, shape, stability, and surface properties of the nanoparticles, the primary methods of characterization of silver nanoparticles are described.

**KEYWORDS:** Microalgae, silver nanoparticles, SEM, Mountain 8 Graphical tool, Micro valley.

### INTRODUCTION

The synthesis of nanoparticles has become the matter of great interest in recent times due to its various advantageous properties, including high sensitivity biomolecule detection and diagnosis<sup>[4]</sup>, tissue engineering,<sup>[2]</sup> antimicrobials<sup>[1]</sup> and therapies, catalysis, and microelectronics.<sup>[3]</sup> However, utilizing metal oxide nanoparticles,<sup>[5]</sup> can have a lot of negative effects on human health. Since the chemical processes used in the production of nanomaterial's produce a significant number of hazardous byproducts,<sup>[6]</sup> the development of novel chemical or physical approaches has led to environmental contaminations Using the scanning

electron microscope (SEM), individual particles and groups of particles can be visualized.<sup>[7]</sup> Here, we used SEM combined with Digital surf: Mountain 8 graphical software to characterize silver nanoparticles and analyze the surface morphology. SEM is a surface imaging technique, capable of fully resolving various particle sizes, size distributions, forms of nanomaterial, and the surface morphology of the produced particles at the micro and nanoscale.<sup>[8]</sup> Using SEM, we can probe the morphology of particles and and counting the particles by using specific software.<sup>[9]</sup>

### Applications of Nanotechnology

Nanotechnologies have an ability to make the existing medical applications cheaper and easier.<sup>[10]</sup> Modern medicine relies heavily on nanotechnology to treat a variety of pathological and metabolic problems, including inflammatory, arthritic, tumour<sup>[11]</sup>, HIV<sup>[12]</sup>, and liver diseases.<sup>[13]</sup> Nanotechnology play a prominent role in the Tissue Engineering, when conspiring the scaffolds, researchers try to mimic the nanoscale features of a Cell's environment to express its differentiation down a suitable lineage and synthesis of regenerated damaged tissue are supported to the growth of bone<sup>[14]</sup>, biomedical engineering scientist may mimic osteoclast resorption pits. Bone reabsorption is a process that breaks down the osteoclasts cells and releases the minerals and proceeds to transfer of calcium from bone tissue to the blood. Nanotechnology which applied in the automobile industries<sup>[16]</sup> use to develop the nanomaterial and diesel engines with cleaner exhaust fumes. Nowadays, Platinum act as a diesel engine catalyst are coupled with diesel particulate filter to carry out the reduction reaction to achieve the C<sub>3</sub>H<sub>6</sub>OH, CO and NH utilization conversion achieved to minimal 60% and exhaust particulate come out from the engine. The platinum

nanoparticle are played role in the clean of exhaust fume and cerium oxide<sup>[17]</sup> also act as a fuel catalyst. Synthesized titanium dioxide<sup>[18]</sup> containing nanoparticles are used in the preparation of sunscreen and lotion, cosmetics products, surface coatings and some food products, Carbon allotropes used to produce gecko tape-adhesive tape, Agricultural Packaging, Aluminum Foil, Apparel Packaging, Blister Cards, and Bottles Cans. Silver materials<sup>[19]</sup> are used in food packaging, cloth manufacturing, disinfectants and household appliances. Zinc oxide<sup>[20]</sup> is used in sunscreens preparation and cosmetics industries, surface coatings, synthetic paints and outdoor furniture varnish. Nanomaterial applications in sports, to allow the manufacture tennis balls to last longer, golf balls<sup>[21]</sup> to fly straighter and even bowling balls to become more durable and have a harder surface. Pants, shirt, socks and other textile materials are infused with nanotechnology so that they will last longer and keep people cool in the summer. Plasters or dressing cloth are being infused with silver nanoparticles to heal cuts faster. Nanoparticles play a role in silicon industries to develop a personal computers<sup>[22]</sup> and electronic device may become cheaper and strong.

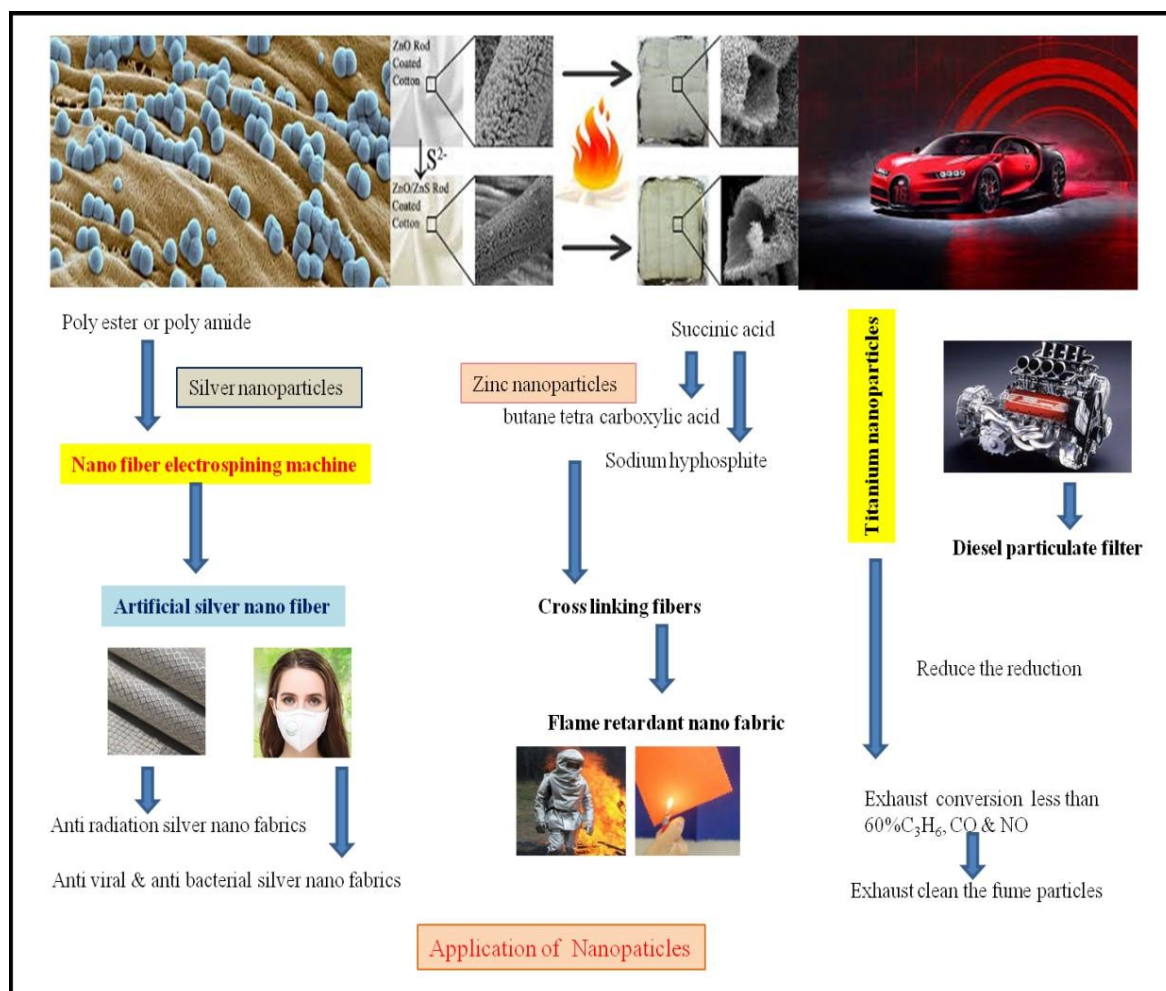


Figure 1: Application of Nanoparticles in textile, mechanical and space research.

## MATERIALS AND METHODS

### Scanning Electron Microscopy Technique (SEM): sample preparation

The Jagna-Karcz method for SEM sample preparation requires for a number of solutions, including phosphate buffer A [ $\text{Na}_2\text{HPO}_4 \cdot 12 \text{H}_2\text{O}$  - 35.82 g/500ml or  $\text{Na}_2\text{HPO}_4 \cdot 2\text{H}_2\text{O}$  -17.8 g/500ml], phosphate buffer B

[ $\text{NaH}_2\text{PO}_4 \cdot 2 \text{H}_2\text{O}$  - 15.6 g/500ml or  $\text{NaH}_2\text{PO}_4 \cdot \text{H}_2\text{O}$  - 13.6 g/500ml] and 3% glutaraldehyde [50 ml 0.2 M phosphate solution + 12 ml 25% glutaraldehyde + 38ml distilled water]. Different steps, including fixation washing, post fixation washing, dehydration critical point drying, and metal coating, are included in the process for preparing biological material.

**Table 1: Scanning Electron Microscopy Sample Fixation Method.**

Step	Process	Compounding
Step 1	Fixation	Immerse the sample in 3% Glutaraldehyde buffered with 0.1 M Phosphate buffer at room temperature or 0-4°C (2-4 hours, maximum 24-48hours).
Step 2	Washing	Rinse the tissue with 0.1 M Phosphate buffer pH=7.2 - (3 x 10min.).
Step 3	Post-Fixation	Immerse sample in 1-2% Osmium Tetroxide in 0.1 M Phosphate buffer, pH=7.2 (2-4 hours) at room temperature and in a light tight container. 1-2% Osmium Tetroxide Solution: (1%) - 0.25g $\text{OsO}_4$ in 25 ml 0.1 M Phosphate buffer (12.5 ml 0.2M Phosphate solution + 12.5 ml distilled water) or 2% Osmium Tetroxide Solution: 0.25g $\text{OsO}_4$ in 12.5 ml 0.1 M Phosphate buffer (6.25 ml 0.2M Phosphate solution + 6.25 ml distilled water).
Step 4	Washing	In 0.1 M Phosphate buffer pH=7.2 (3 times for 10 minutes).
Step 5	Dehydration	In a graded ethanol or acetone solutions in water – 30%, 50%, 70% (can store tissue in 70% ethanol), 80%, 90%, 96%, 100% for 5-15 minutes each); 2 times in 100% ethanol or acetone (15-30 minutes each).
Step 6	Dehydration	In a graded ethanol or acetone solutions in water – 30%, 50%, 70% (can store tissue in 70% ethanol), 80%, 90%, 96%, 100% for 5-15 minutes each); 2 times in 100% ethanol or acetone (15-30 minutes each).
Step 7	Critical Point Drying	-
Step 8	Mounting	Mount on specimen stub with carbon/silver paste or graphite
Step 9	Metal coating	Coat with gold/palladium alloy
Step 10	Viewing sample	Store stubs in desiccators

### Studies of biogenic nanoparticle 2D and 3D topographical blueprint

The extracted biogenic silver nanoparticles and its characterization studies were analyzed by using surface analyzing software. The Mountain -8-expert graphical tool play an important role in structural prediction, Contour lines, Micro valley studies, extract profile study, area of hole. Down load the software installation file from: [digital.surf.com/support/software.updates](http://digital.surf.com/support/software.updates). Unzip the file then double click on the Autorun.exe to begin the installation process. Choose install surface analysis software and follow the on-screen installation of the installation wizard.

## RESULT AND DISCUSSION

### Scanning Electron Microscopy (SEM) - [AgNPs]

The green synthesis of silver nanoparticles was demonstrated by using SEM. This SEM images confirmed that the metal particles are present in nanosize. The SEM micrograph of the synthesized silver nanoparticles were magnified in 11500X at an accelerating voltage of 10 kV and the particles were spherical shaped with an average diameter of 60nm–344nm. The SEM images show small scattered structure

of biosynthesized silver nanoparticles which agglomerates in to larger size. It is also can be correlated with the observed broad area of the absorbance peak. The bio-organic compounds in the microalgal extract seems to act as a ligand which effectively stabilizes the formed silver nanoparticles. The silver nanoparticles shape and size were photographed by using SEM (Figure: 2, 3 and 4).

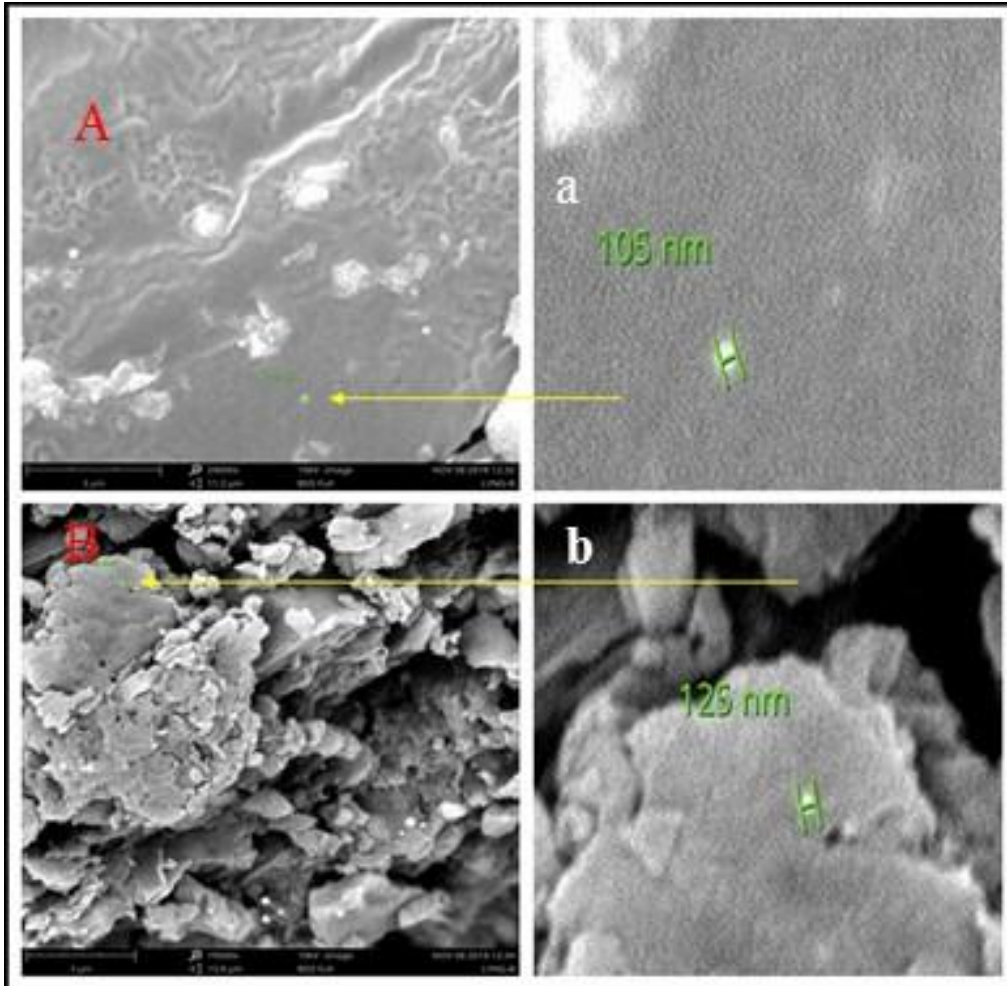


Figure 2: SEM images of biogenic silver nanoparticle from *Lyngbya* sp. (A, B: arrow marked) and (a, b: sizes of the nanoparticles).

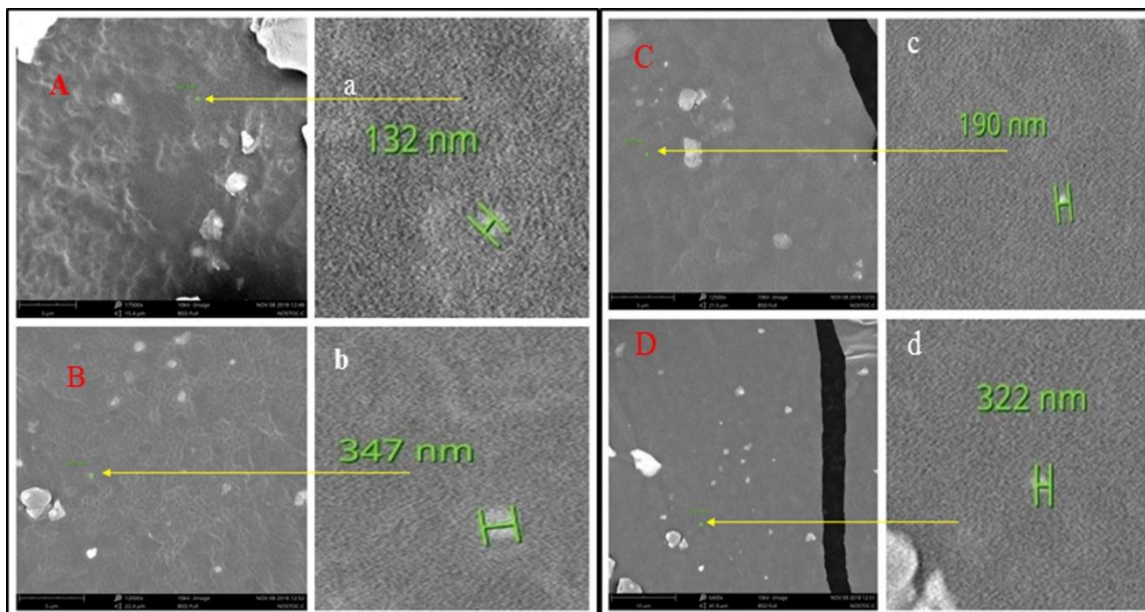


Figure 3: SEM images of biogenic silver nanoparticle from *Nostoc* sp. (A, B, C and D: arrow marked) and (a, b, c and d: sizes of the nanoparticles).

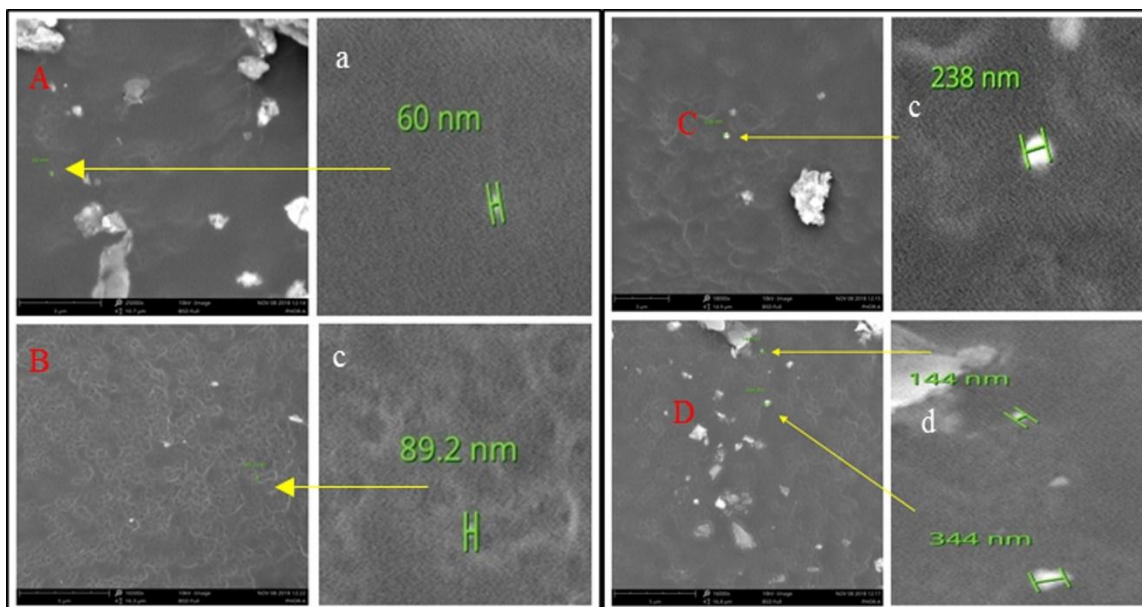


Figure 4: SEM images of biogenic silver nanoparticle from *phormidium sp.* (A, B, C and D: arrow marked) and (a, b, c and d: sizes of the nanoparticles).

**Dispersive X-ray spectrometer (SEM-EDX EDAX - AgNPs)**

The scanning electron microscope with energy dispersive X-ray spectrometer (SEM-EDX) was employed to determine the silver concentration of the nanoparticles. Energy Dispersive Analysis of silver nanoparticles gives qualitative and quantitative status of elements that may be involved in the formation of silver nanoparticles. The peak shows silver region at 3Kev which is typical for the

absorption of metallic silver nanocrystalline due to surface Plasmon resonance. A silver concentration of 41.26%, 36.53% and 63.17% in the *Nostoc sp.*, *Lyngbya sp.*, and *Phormidium sp.*, were detected after incubation for 48 hrs. The graph also shows the presence of potassium and sodium in the EDX picture of silver nanoparticles (Figure: 5, 6 and 7). This is probably due to the presence of substrate over which the NP sample was held during SEM microscopy.

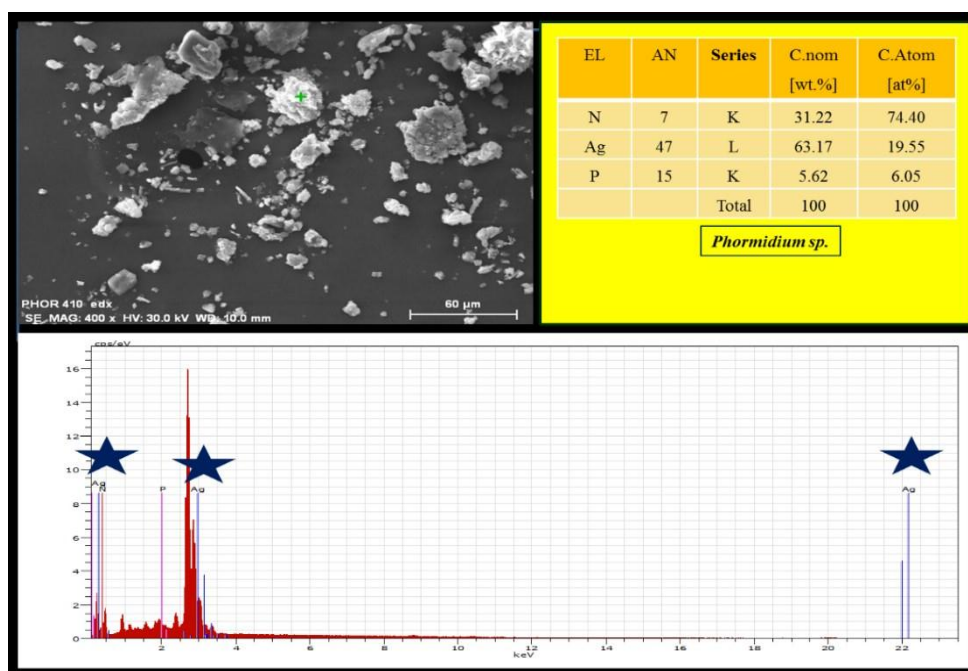


Figure 5: EDAX spectra of Silver Nanoparticles Synthesized in *Phormidium sp.*

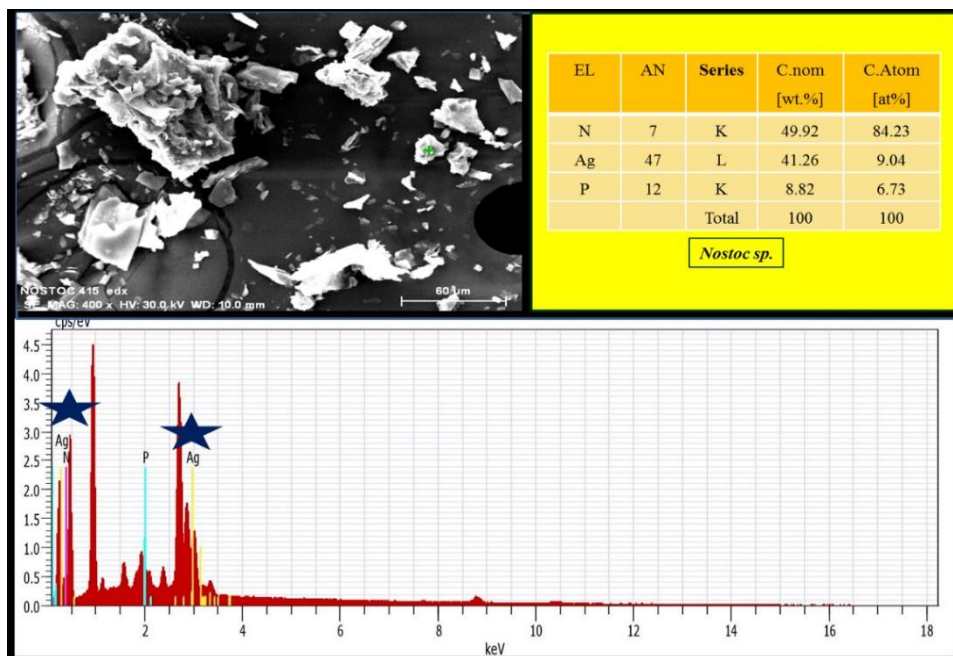


Figure 6: EDAX spectra of Silver Nanoparticles Synthesized in *Nostoc sp.*

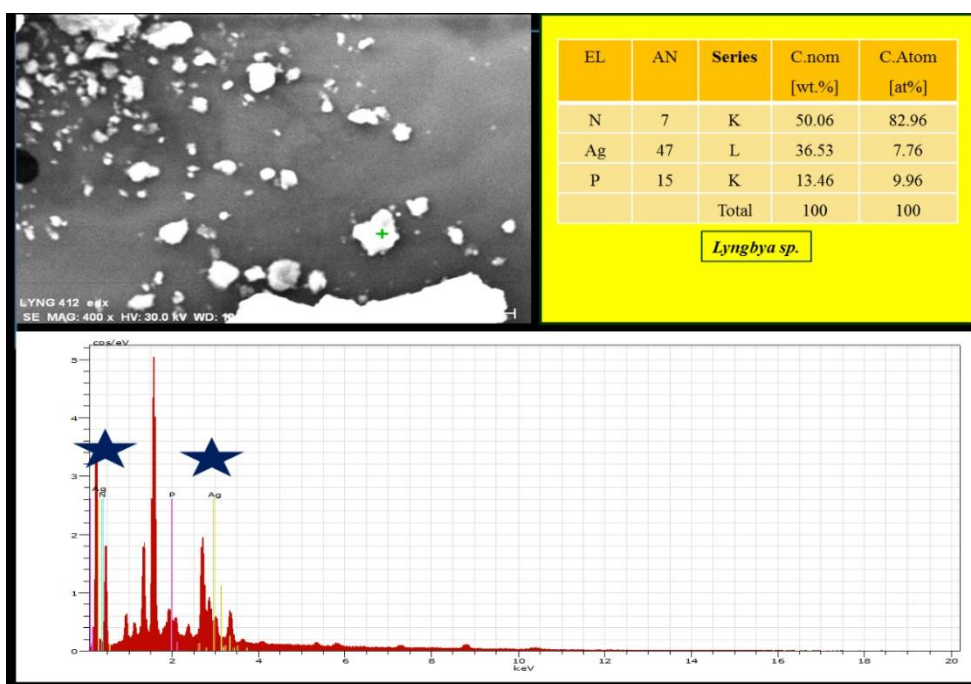


Figure 7: EDAX spectra of Silver Nanoparticles Synthesized in *Lyngbya sp.*

**Convert image in to surface: 3 D Luminance**

The 3D luminance was a practical method to create biogenic silver nanoparticle surface roughness measurement in SEM that was to build the stereographic portrait image. It includes, taking 2 portraits with various tilt angles which was used to calculate the 3D image of the surface and used for any kind of surface analysis. The scanning electron microscopy (SEM) was a surface-imaging technique that produces images of a sample by scanning and focused beam of electrons. The incident electron was attracted with the sample and generate electron signals to reflect the direct image and the atomic composition of the scanned surface. The incident

electrons cause emissions of elastically back scattered electrons (BS), secondary in elastically scattered electrons, and characteristic X-rays from the atoms on the sample surface. Detection of the secondary electrons is the most common mode in SEM. A different kind of topographical surface features can be identified and surface is further subjected in Gaussian filtering to reduce the S-L surface noise. (Figure: 8, 9 and 10). Hi-tech machine processing MOUNTAIN MAPS programming: 3D Luminance surface of biogenic nanoparticle from a: *Nostoc sp.*, b: *Lyngbya sp.*, c: *Phormidium sp.* (secondary profile: Arrows represent the extracted profile are shown in Table: 2).

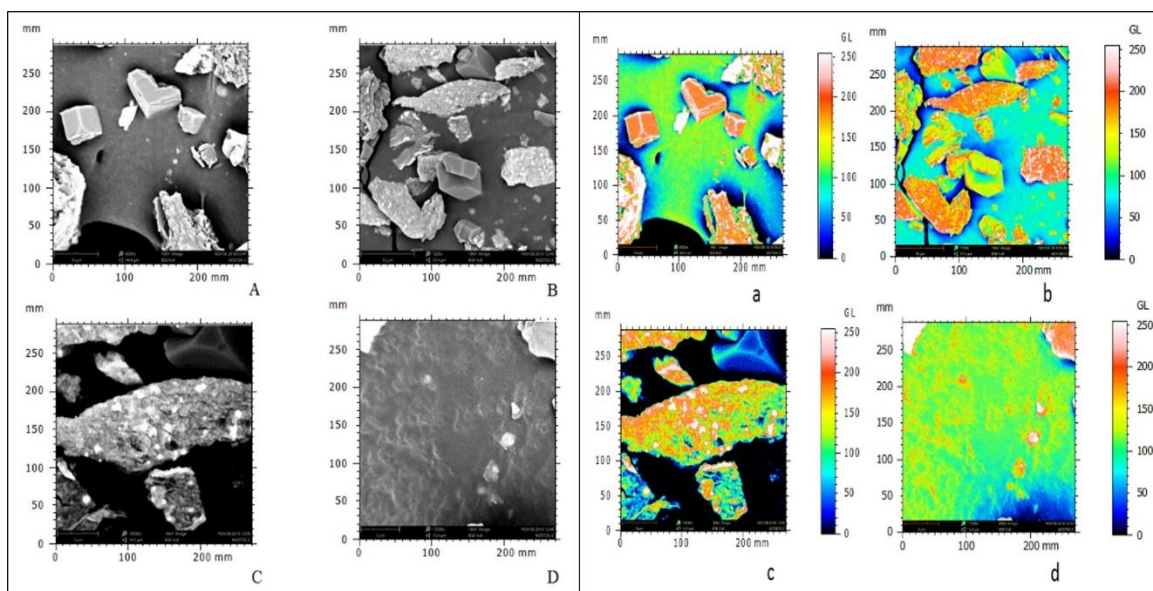


Figure 8: SEM images of biogenic surface silver nanoparticle from *Nostoc* sp. (Left side A, B, C and D: black and white) and Hitech machine processing MOUNTAIN MAPS programming used to create the 3D Luminance of biogenic surface silver nanoparticle from *Nostoc* sp. (Extracted primary profile : Right side a, b, c and d: colour).

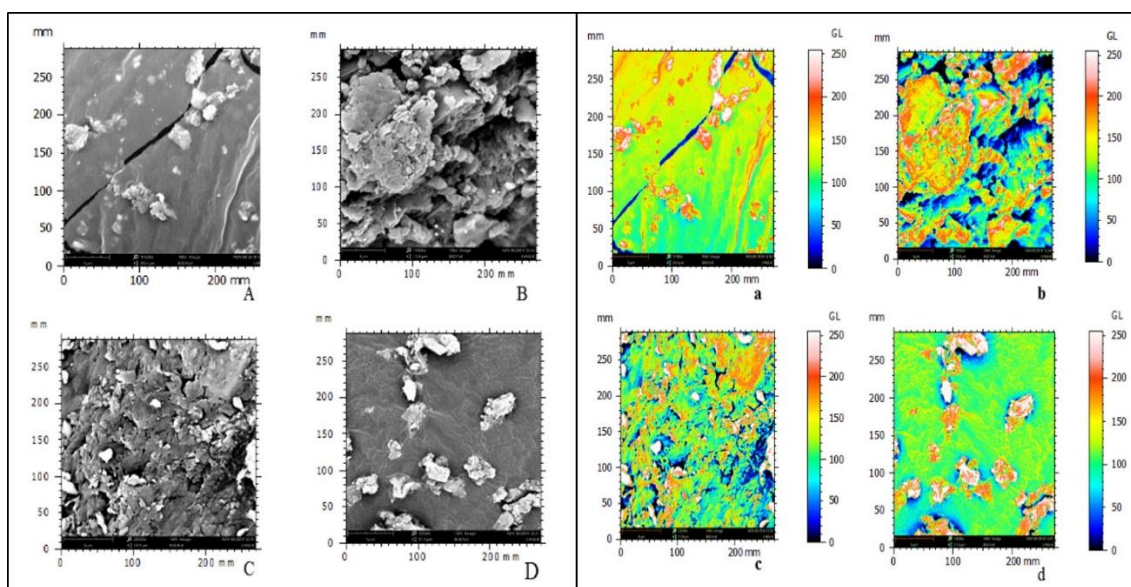


Figure 9: SEM images of biogenic surface silver nanoparticle from *Lyngbya* sp. (Left side A, B, C and D: black and white) and Hitech machine processing MOUNTAIN MAPS programming used to create the 3D Luminance of biogenic surface silver nanoparticle from *Lyngbya* sp. (Extracted primary profile : Right side a, b, c and d: colour).

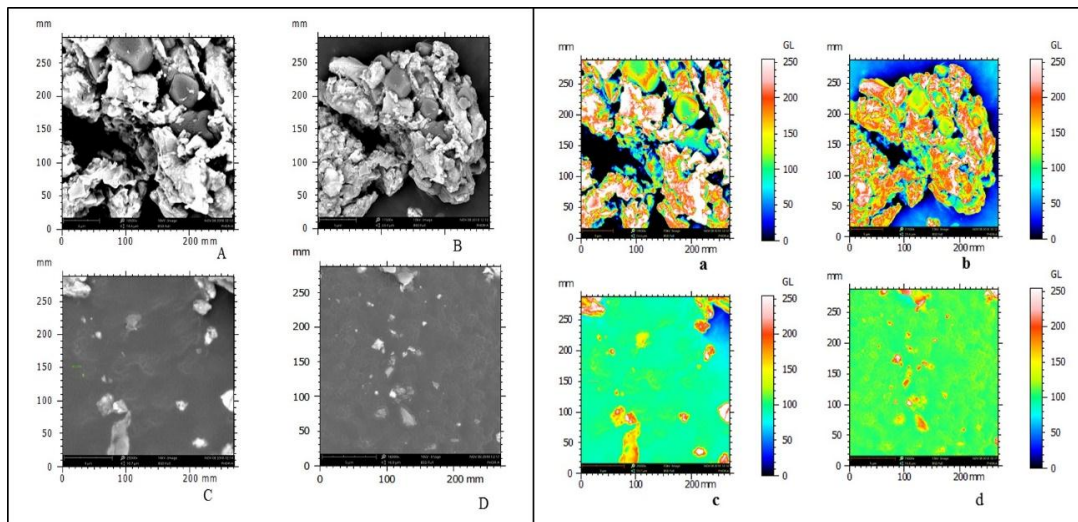


Figure 10: SEM images of biogenic surface silver nanoparticle from *Phormidium* sp. (Left side A, B, C and D: black and white) and Hitech machine processing MOUNTAIN MAPS programming used to create the 3D Luminance of biogenic surface silver nanoparticle from *Phormidium* sp. (Extracted primary profile : Right side a, b, c and d: colour).

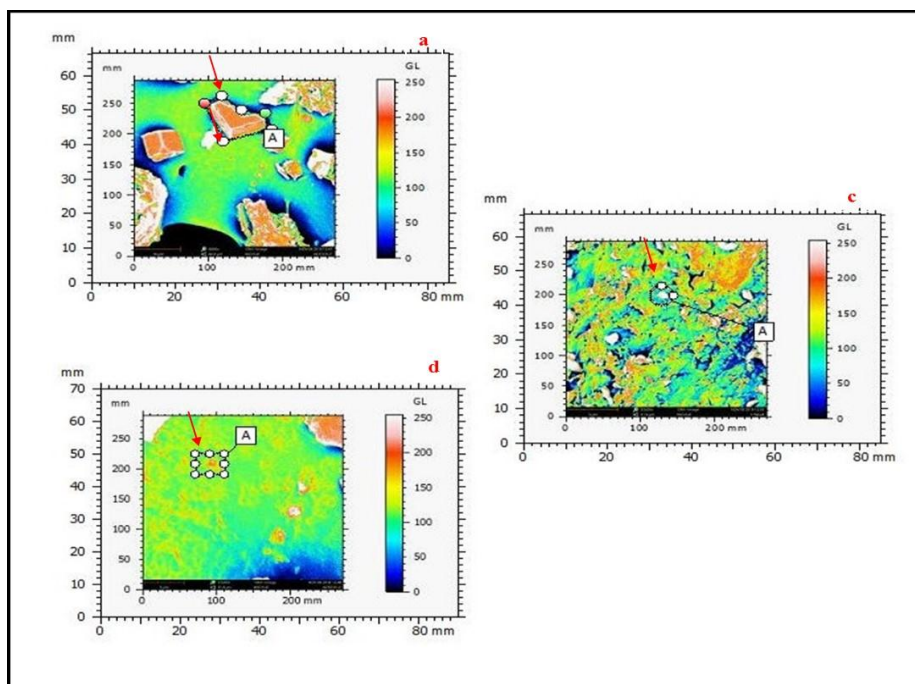


Figure 11: Hi-tech machine processing MOUNTAIN MAPS programming: 3D Luminance surface of biogenic nanoparticle from *Nostoc* sp., *Lyngbya* sp., *Phormidium* sp. (Extracted secondary profile: a, c, d).

Table 2: MOUNTAIN MAPS programming: 3D Luminance surface of biogenic nanoparticle from a: *Nostoc* sp., b: *Lyngbya* sp., c: *Phormidium* sp.

MOUNTAIN MAPS: Extracted surface profile parameters	<i>Nostoc</i> sp. (a)	<i>Lyngbya</i> sp. (c)	<i>Phormidium</i> sp. (d)
Projected area	116.4mm <sup>2</sup>	25.27mm <sup>2</sup>	17.47 mm <sup>2</sup>
perimeter	45.69 mm	17.82mm	14.87 mm
Minimum Diameter	9.299 mm	-	-
Angle of minimum diameter	83.00°	-	-
Maximum diameter	15.79.0 mm	-	-
Angle of maximum diameter	-18..0°	-	-
Equivalent radius	6.087 mm	2.836 mm	2.388 mm
Equivalent diameter	12.17 mm	5.673 mm	4.717 mm

Mean diameter	9.345 mm	-	-
Form factor	0.7005	1.000	0.9931
Aspect ratio	1.698	-	-
Roundness	0.5321	-	-
Compatchness	0.7294	-	-
Orientation	154.6°	3.901°	0.000°
Length	17.78 mm	5.281mm	5.049 mm
Width	11.81 mm	6.039 mm	4.406mm
Elongation	0.3358	0.1434	0.1272
X-extent	16.40 mm	6.045 mm	5.292mm
Y-extent	13.46 mm	5.828mm	4.763mm
Convexity	0.9902	1.000	1.000
Solidity	0.9254	1.000	1.000
X of geometric center	34.28 mm	32.82 mm	28.71 mm
Yof geometric center	47.18mm	42.80 mm	45.54 mm
Maximum caliber	17.78 mm	8.022 mm	6.701 mm

### Contour map: surface of biogenic nanoparticle

The surface roughness have been usually a detrimental by-product of all machining processes. These modernized research work which was applied in digital image processing system of MOUNTAIN MAPS programming to measure, generate a 3-D contour plot of nanoparticle surface roughness, The acquired RGB images were deselected, kept their feature ratios intact to standardized the comparison. The gray scale and binary conversions were performed. The peaks and valleys of the surface roughness showed up as bright and dark regions in the grayscale images. The Mountain maps stored each resized image as a 2-D matrix, where each column corresponded to a 'strip' of the image and contained pixel of the image acquisition setup intensity values. The *MOUNTAIN MAP* was a programming and numeric computing platform used by millions of engineers and scientists to analyze data, develop algorithms, and create models (Figure: 12-14). Hi-tech machine processing MOUNTAIN MAPS programming used to create the Contour map -surface of biogenic nanoparticle from *Nostoc* sp., *Lyngbya* sp., *Phormidium*

sp. and extracted secondary profile: a, c and d, are shown in (Figure: 15 and Table: 3-5).

### Micro valley networks: surface of biogenic nanoparticle

The hi-tech machines process innovative modelling technique was applied in the microvalley network studies of silver nanoparticle surface roughness. The averaged density of valley varies from primary groove to secondary groove. These specific representations of the surface evident that create an abrasion operation procedure to smooth surface with larger number of deeper valleys which causes the increased retention capability. The maximum depth of furrows, mean depth of the furrows and mean density of furrows values was calculated by using software digital surf analysis tool and photographed (Figure:12-14). Hi-tech machine processing MOUNTAIN MAPS programming create the micro valley network: surface of biogenic nanoparticles maximum depth of furrows in *Nostoc* sp., *Lyngbya* sp., *Phormidium* sp. are shown in Table: 6-8.

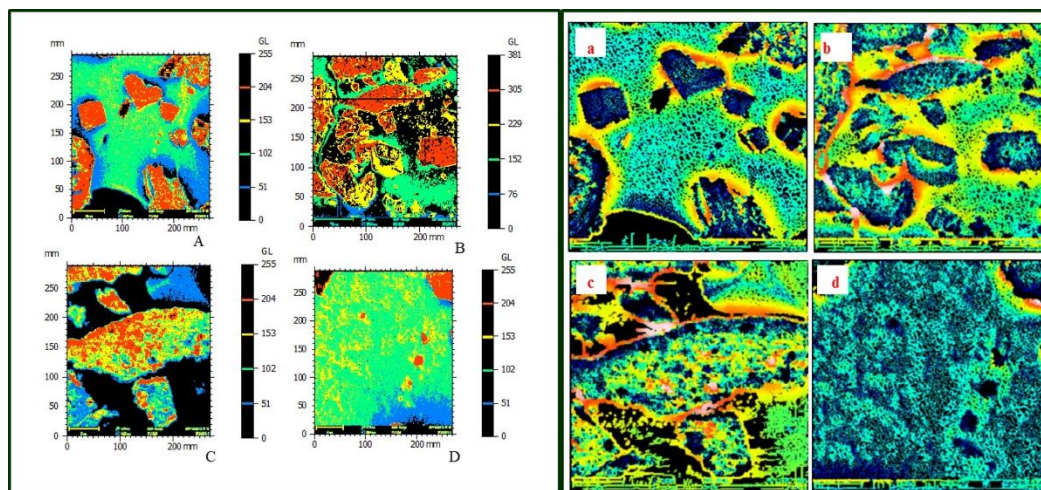


Figure 12: Hi-tech machine processing MOUNTAIN MAPS programming use to create the Contour map: surface of biogenic nanoparticle from *Nostoc* sp. (Left side A, B, C and D: colour) and micro valley network. (Right side a, b, c and d: Shown the furrows).

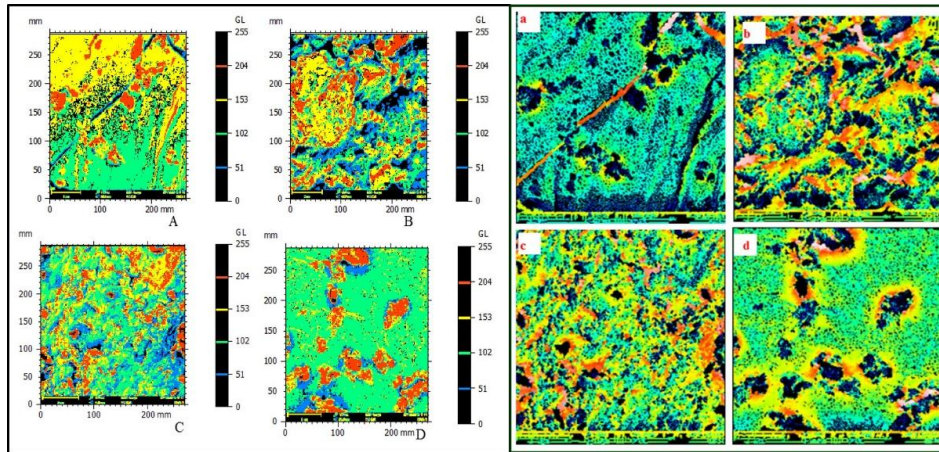


Figure 13: Hi-tech machine processing MOUNTAIN MAPS programming create the Contour map: surface of biogenic nanoparticle from *Lyngbya* sp. (Left side A, B, C and D: colour) and micro valley network. (Right side a, b, c and d: Shown the furrows).

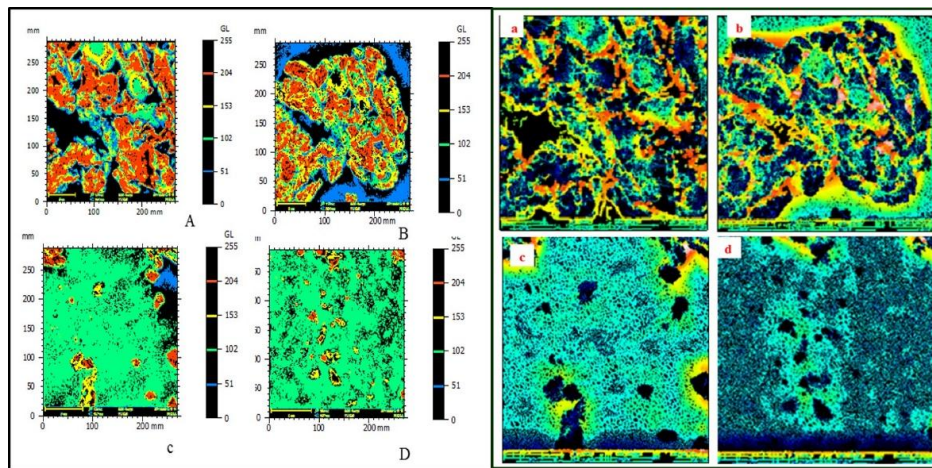


Figure 14: Hi-tech machine processing MOUNTAIN MAPS programming create the Contour map: surface of biogenic nanoparticle from *Phormidium* sp. (Extracted primary profile: Left side A, B, C and D: colour) and micro valley network. (Extracted primary profile: Right side a, b, c and d: Shown the furrows).

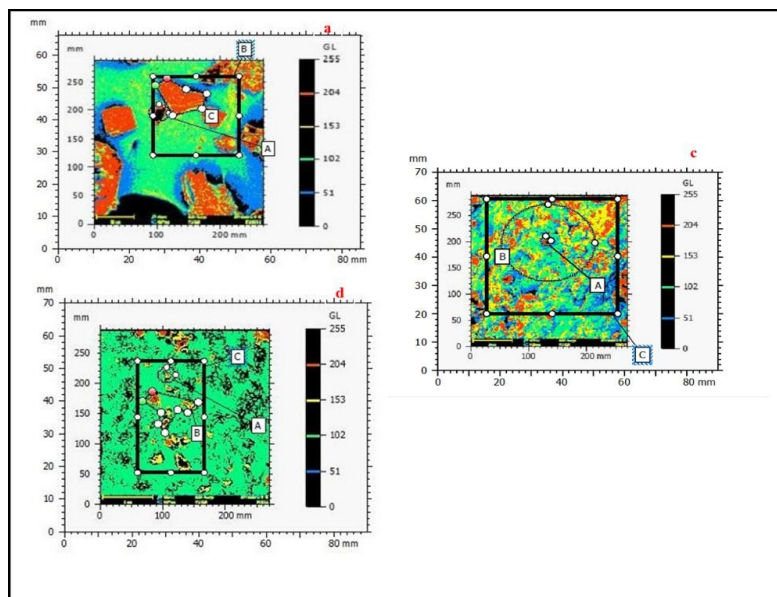


Figure 15: Hi-tech machine processing MOUNTAIN MAPS programming used to create the Contour map - surface of biogenic nanoparticle from *Nostoc* sp., *Lyngbya* sp., *Phormidium* sp. (Extracted secondary profile: a, c, d).

**Table 3: MOUNTAIN MAPS programming used to create the Contour map -surface of biogenic nanoparticle from *Nostoc* sp.**

<b>MOUNTAIN MAPS: Extracted surface profile parameters: <i>Nostoc</i> sp. (a)</b>	<b>L.area :[A]</b>	<b>L.area: [B]</b>	<b>L.area: [c]</b>
Projected area	23.98 mm <sup>2</sup>	597.7 mm <sup>2</sup>	92.91 mm <sup>2</sup>
perimeter	17.37 mm	97.79 mm	14.87 mm
Minimum Diameter	-	24.35	8.134
Angle of minimum diameter	-	1.000	48.00
Maximum diameter	-	34.42	14.81
Angle of maximum diameter	-	45.00	-28.0
Equivalent radius	2.763 mm	13.79 mm	5.438 mm
Equivalent diameter	5.526 mm	27.59 mm	10.88 mm
Mean diameter	-	20.44 mm	8.446 mm
Form factor	0.9989	0.7854	0.7253
Aspect ratio	-	1.414	1.821
Roundness	-	0.6092	0.4840
Compatchness	-	0.7805	0.6957
Orientation	176.7°	0.000°	151.0°
Length	5.982 mm	24.34 mm	14.98 mm
Width	5.037 mm	24.55 mm	10.58 mm
Elongation	0.1580	0.008688	0.2935
X-extent	5.821mm	24.61 mm	14.55 mm
Y-extent	5.821mm	24.61mm	11.91 mm
Convexity	1.000	1.000	0.9963
Solidity	1.000	1.000	0.9412
X of geometric center	28.40 mm	38.85 mm	34.43mm
Yof geometric center	42.22 mm	41.27mm	46.89mm
Maximum caliber	7.821 mm	34.57 mm	0.000 mm

**Table 4: MOUNTAIN MAPS programming used to create the Contour map -surface of biogenic nanoparticle from *Lyngbya* sp., (Extracted secondary profile: c).**

<b>MOUNTAIN MAPS: Extracted surface profile parameters: <i>Lyngbya</i> sp. (c)</b>	<b>L. area :[A]</b>	<b>L. area: [B]</b>	<b>L. area: [c]</b>
Projected area	8.695 mm <sup>2</sup>	638.0 mm <sup>2</sup>	1704 mm <sup>2</sup>
perimeter	10.45 mm	89.71 mm	165.2 mm
Minimum Diameter	-	-	40.48
Angle of minimum diameter	-	-	-90.0
Maximum diameter	-	-	58.27
Angle of maximum diameter	-	-	44.00
Equivalent radius	1.664 mm	14.25 mm	23.29 mm
Equivalent diameter	3.327 mm	28.50 mm	46.58 mm
Mean diameter	-	-	35.12
Form factor	1.000	0.9961	0.7851
Aspect ratio	-	-	1.440
Roundness	-	-	0.6224
Compatchness	-	-	0.7889
Orientation	90.00°	0.02171°	0.000°
Length	3.323 mm	29.98 mm	42.11mm
Width	3.332 mm	27.10 mm	40.48 mm
Elongation	0.002655	0.0959	0.03878
X-extent	3.440 mm	30.16 mm	42.33 mm
Y-extent	3.704 mm	27.52 mm	40.75 mm
Convexity	1.000	1.000	1.000
Solidity	1.000	1.000	1.000
X of geometric center	34.65 mm	35.41 mm	36.69 mm
Yof geometric center	45.86 mm	45.10 mm	40.32 mm
Maximum caliber	4.706 mm	40.41 mm	58.41 mm

**Table 5: MOUNTAIN MAPS programming used to create the Contour map -surface of biogenic nanoparticle from *Phormidium* sp., (Extracted secondary profile: d).**

<b>MOUNTAIN MAPS: Extracted surface profile parameters: <i>Phormidium</i> sp, (d)</b>	<b>L. area: [A]</b>	<b>L. area: [B]</b>	<b>L. area: [c]</b>
Projected area	19.57 mm <sup>2</sup>	82.81mm <sup>2</sup>	678.9 mm <sup>2</sup>
perimeter	15.73 mm	47.30 mm	108.1 mm
Minimum Diameter	-	7.163	19.86
Angle of minimum diameter	-	39.00	0.000
Maximum diameter	-	14.04	39.47
Angle of maximum diameter	-	-13.0	-60.0
Equivalent radius	2.496 mm	5.134 mm	14.70 mm
Equivalent diameter	4.992 mm	10.27 mm	29.40 mm
Mean diameter	-	7.955 mm	20.44 mm
Form factor	0.9936	0.4650	0.7303
Aspect ratio	-	1.960	1.987
Roundness	-	0.4440	0.5346
Compatchness	-	0.6664	0.7312
Orientation	0.03164°	1751.5°	90.00°
Length	5.328 mm	16.512 mm	34.18 mm
Width	4.677 mm	11.86 mm	19.86 mm
Elongation	0.1222	0.2814	0.4189
X-extent	5.556 mm	16.93 mm	20.11 mm
Y-extent	5.027 mm	12.70 mm	34.66 mm
Convexity	1.000	0.9223	1.000
Solidity	1.000	0.7814	1.000
X of geometric center	30.32 mm	30.73 mm	31.54 mm
Yof geometric center	48.08 mm	38.23 mm	35.20 mm
Maximum caliber	7.090 mm	16.65 mm	39.53 mm

**Table 6: Hi-tech machine processing MOUNTAIN MAPS programming create the micro valley network: surface of biogenic nanoparticles maximum depth of furrows in *Nostoc* sp.**

<b>Information: Micro valley network: <i>Nostoc</i> sp.</b>	<b>a</b>		<b>B</b>		<b>C</b>		<b>d</b>	
Parameters	value	unit	value	unit	value	unit	value	unit
Maximum depth of furrows	314.7	GL	237.6	GL	253.5	GL	190.5	GL
Mean depth of furrows	109.9	GL	89.80	GL	102.7	GL	51.63	GL
Mean density of furrows	3.162	cm/cm <sup>2</sup>	3.427	cm/cm <sup>2</sup>	2.626	cm/cm <sup>2</sup>	3.391	cm/cm <sup>2</sup>

**Table 7: Hi-tech machine processing MOUNTAIN MAPS programming create the micro valley network: surface of biogenic nanoparticles maximum depth of furrows in *Lyngbya* sp.**

<b>Information: Micro valley network: <i>Lyngbya</i> sp.</b>	<b>a</b>		<b>B</b>		<b>C</b>		<b>d</b>	
Parameters	value	unit	value	unit	value	unit	value	unit
Maximum depth of furrows	226.2	GL	238.7	GL	272.8	GL	251.4	GL
Mean depth of furrows	70.81	GL	94.04	GL	115.1	GL	105.9	GL
Mean density of furrows	3.324	cm/cm <sup>2</sup>	3.070	cm/cm <sup>2</sup>	3.257	cm/cm <sup>2</sup>	3.517	cm/cm <sup>2</sup>

**Table 8: Hi-tech machine processing MOUNTAIN MAPS programming create the micro valley network: surface of biogenic nanoparticles maximum depth of furrows in *Phormidium* sp.**

Information: Micro valley network: <i>Phormidium</i> sp.	a		B		C		d	
Parameters	value	unit	value	unit	value	unit	value	unit
Maximum depth of furrows	316.5	GL	264.0	GL	167.3	GL	138.4	GL
Mean depth of furrows	110.7	GL	96.31	GL	54.99	GL	37.54	GL
Mean density of furrows	2.551	cm/cm <sup>2</sup>	3.106	cm/cm <sup>2</sup>	3.296	cm/cm <sup>2</sup>	3.483	cm/cm <sup>2</sup>

## CONCLUSION

The green synthesis of silver nanoparticles was demonstrated by using SEM. This SEM images confirmed that the metal particles are present in nanosize. The SEM micrograph, synthesized silver nanoparticles in the 11500× magnification and at an accelerating voltage of 10 kV, the particles were spherical shaped with an average diameter of 60nm–344nm. The SEM images show small scattered structure of biosynthesized silver nanoparticles which agglomerates in to larger size. It is also can be correlated with the observed broad area of the absorbance peak. The bio-organic compounds in the microalgal extract seems to act as a ligand which effectively stabilizes the formed silver nanoparticles. The silver nanoparticles shape and size were photographed by using SEM. The scanning electron microscope with energy dispersive X-ray spectrometer (SEM-EDX) was employed to determine the silver concentration of the nanoparticles. Energy Dispersive Analysis of silver nanoparticles gives qualitative and quantitative status of elements that may be involved in the formation of silver nano particles. The peak shows silver region at 3Kev which is typical for the absorption of metallic silver nanocrystalline due to surface Plasmon resonance. A silver concentration of 41.26%, 36.53% and 63.17% in the *Nostoc* sp., *Lyngbya* sp., and *Phormidium* sp., were detected after incubation for 48 hrs. The graph also shows the presence of potassium and sodium in the EDX picture of silver nanoparticles. This result was well supported by the previous findings of SEM and EDAX spectra of synthesized silver nanoparticles in microalgae.

A different type of topographical surface features can be detected [Matej Harcarik and Robert Jankovych, (2016)]. The projection beyond the center plane was referred to as hills [represented in green colour], and their maximum altitude was called peaks [represented in orange colour]. The areas under the center plane were called as a dale [represented in blue colour], and their lowest valley points being pits [represented in black colour]. The S-L surface were further subject into Gaussian filtering [ISO 25178-2:2012]. The Gaussian filters play a major role in filtering the different type of surfaces. The nanoparticle surface characterization was studied by using linear Gaussian filters. It can be applied to the input surface by calculating the entanglement of measured surface with a Gaussian and Laplacian of Gaussian weighting functions

for robust feature-based tracking. NumPy used to perform a wide variety of mathematical operations such as algorithm, matrix array. It promotes the number of mathematical library functions, which was used to achieve the hi-tech machine processing Moutain MAPS programming used to retrieve the surface model- 3D Luminance of biogenic silver nanoparticle from *Nostoc* sp., *Lyngbya* sp., and *phormidium* sp. A different type of topographical surface features can be detected. The Gaussian filters play a major role in filtering the different type of surfaces. The acquired RGB images were deselected, kept their feature ratios intact to standardize the comparison. The gray scale and binary conversions were performed. The peaks and valleys of the surface roughness showed up as bright and dark regions in the grayscale images. Pinpoint the surface of contour line were far away [represented as a-Maximum peaks in orange color, black color-pit], and contour lines close eath other [representing in yellow-hills, blue-dales] The Moutain maps representation showed the maximum peak, pit, hill, and dale from *Nostoc* sp., *Lyngbya* sp., and *phormidium* sp. The dominant wavelength, maximum roughness and maximum amplitude were calculated from the biogenic silver nanoparticle surface in *Nostoc* sp., *Lyngbya* sp., and *Phormidium* sp. The hi-tech machine processing Moutain MAPS programming used to retrieve the surface model-3D Luminance of biogenic silver nanoparticle from *Nostoc* sp., *Lyngbya* sp., and *Phormidium* sp.

## ACKNOWLEDGMENTS

The authors gratefully acknowledge the Dr. Mageshkumar, CLRI-center for analysis, testing evaluation and reporting services [CATERS].

## Conflict of interest

Conflict of interest declared none.

## REFERENCES

1. Chetan Pandit, Arpita Roy, Suresh Ghotekar, Ameer Khusro, Mohammad Nazmul Islam, Talha Bin Emran, Siok Ee Lam, Mayeen Uddin Khandaker, David Andrew Bradley. Biological agents for synthesis of nanoparticles and their applications, Journal of King Saud University-Science, 2022; 34(3): 101869.
2. Velusamy P, Kumar GV, Jeyanthi V, Das J, Pachaiappan R. Bio-Inspired Green Nanoparticles:

- Synthesis, Mechanism, and Antibacterial Application. *Toxicological Research*, 2016; Apr; 32(2): 95-102. doi: 10.5487/TR.2016.32.2.095. Epub 2016 Apr 30. PMID: 27123159.
3. De M, Ghosh P S and Rotello V M 2008 *Adv. Mater.* 20 4225.
  4. Lee SH, Jun BH. Silver Nanoparticles: Synthesis and Application for Nanomedicine. *International Journal of Molecular Sciences*, 2019; 20(4): 865. doi: 10.3390/ijms20040865. PMID: 30781560.
  5. Ray PC, Yu H, Fu PP. Toxicity and environmental risks of nanomaterials: challenges and future needs. *Journal of environmental science and health. Part C, Environmental carcinogenesis & ecotoxicology reviews*, 2009; 27(1): 1-35. doi: 10.1080/10590500802708267. PMID: 19204862.
  6. FoziaHaqueKhan, Chemical Hazards of Nanoparticles to Human and Environment (A Review), *Oriental journal of chemistry*, 2013; 29(4): 1399-1408.
  7. Mahsa Ydollahi, Hamed Ahari1 and Amir Ali Anvar, Antibacterial activity of silver-nanoparticles against *Staphylococcus aureus*. *African Journal of Microbiology Research*, 2016; 10(23): 850-855. doi: 10.5897/AJMR2016.7908.
  8. Bryan Calderón-Jiménez, Monique E. Johnson, Antonio R. Montoro Bustos, Karen E. Murphy, Michael R. Winchester and José R, Silver Nanoparticles: Technological Advances, Societal Impacts, and Metrological Challenges, *Frontiers in Chemistry*, 2017; 5: 6. doi: 10.3389/fchem.2017.00006.
  9. Katarzyna Odziomek, Daniela Ushizima, Przemyslaw Oberbek, Tomasz Puzyn1, Maciej Haranczyk, Scanning electron microscopy image representativeness: Morphological data on nanoparticles, *Article in Journal of Microscopy*, 2016; doi:10.1111/jmi.12461.
  10. Anna Pratima Nikalje. Nanotechnology and its Applications in Medicine *Article in Medicinal Chemistry*, 2015; 5: 2. doi:10.4172/2161-0444.1000247.
  11. Patra JK, Das G, Fraceto LF, Campos EVR, Rodriguez-Torres MDP, Acosta-Torres LS, Diaz-Torres LA, Grillo R, Swamy MK, Sharma S, Habtemariam S, Shin HS. Nano based drug delivery systems: recent developments and future prospects. *Journal of Nanobiotechnology*, 2018; 16(1): 71. doi: 10.1186/s12951-018-0392-8. PMID: 30231877; PMCID: PMC6145203.
  12. Parboosing R, Maguire GE, Govender P, Kruger HG. Nanotechnology and the treatment of HIV infection. *Viruses*, 2012; 4(4): 488-520. doi: 10.3390/v4040488. PMID: 22590683.
  13. Bai X, Su G, Zhai S. Recent Advances in Nanomedicine for the Diagnosis and Therapy of Liver Fibrosis. *Nanomaterials (Basel)*, 2020; 10(10): 1945. doi: 10.3390/nano10101945. PMID: 33003520.
  14. Griffin MF, Kalaskar DM, Seifalian A, Butler PE. An update on the Application of Nanotechnology in Bone Tissue Engineering. *The open orthopaedics journal*, 2016; 10: 836-848. doi: 10.2174/1874325001610010836. PMID: 28217209; PMCID: PMC5299580.
  15. S S Chavan, S V Dubal. Nanotechnology Applications in Automobiles: Comprehensive Review Of Existing Data, *International Journal of Modern Trends in Engineering and Science*, ISSN: 2348-3121.
  16. Hongbo Shi, Ruth Magaye, Vincent Castranova and Jinshun Zhao. Titanium dioxide nanoparticles: a review of current toxicological data, *Particle and Fibre Toxicology*, 2013; 10: 15.
  17. V. Arul Mozhi Selvan, R. B. Anand and M. Udayakumar, Effects of cerium oxide nanoparticle addition in diesel and diesel-biodiesel-ethanol blends on the performance and emission characteristics of a ci engine. *ARPN Journal of Engineering and Applied Sciences*, 2009; 4(7): ISSN 1819-6608.
  18. Joanna Musial, Rafal Krakowiak, Dariusz T. Mlynarczyk, Tomasz Goslinski and Beata J. Stanis, Titanium Dioxide Nanoparticles in Food and Personal Care Products-What Do We Know about Their Safety?. *Nanomaterials*, 2020; 10: 1110.
  19. Deshmukh SP, Patil SM, Mullani SB, Delekar SD. Silver nanoparticles as an effective disinfectant: A review. *Materials science & engineering. C, Materials for biological applications*, 2019; 97: 954-965. doi: 10.1016/j.msec.2018.12.102. PMID: 30678983; PMCID: PMC7127744.
  20. Clar JG, Platten WE 3rd, Baumann E, Remsen A, Harmon SM, Rodgers K, Thomas TA, Matheson J, Luxton TP. Release and transformation of ZnO nanoparticles used in outdoor surface coatings for UV protection. *The Science of the total environment*, 2019; 670: 78-86. doi: 10.1016/j.scitotenv.2019.03.189. PMID: 30903905.
  21. Alan Smith. Nanotechnology Does It Have a Sporting Chance? *CHEMISTRY International*, 2006.
  22. Sachin Kumar, Garima Pant, Vibhor Sharma, Pooja Bisht, *Nanotechnology in Computers International Journal of Information & Computation Technology*, 2014; 4(15): 1597-1603.